ISBN: 978-3-95450-219-6 ISSN: 2226-0366 doi: 10.18429/JACoW-LINAC2024-THPB089

DEVELOPMENT OF PLASMA PROCESSING OF 1.3 GHZ SUPERCONDUCTING RADIOFREQUENCY CAVITIES AT TRIUMF

D. Hedji[1, 2 †], R. E. Laxdal[1, 2], P. Kolb[1], Z. Yao[1], V. Zvyagintsev[1], T. Junginger[2]
[1]TRIUMF, Vancouver, B.C., Canada
[2]Department of Physics and Astronomy, University of Victoria, Victoria, B.C., Canada

Abstract

Superconducting Radio Frequency (SRF) technology is a key component in many particle accelerators operating in a continuous wave, or high duty cycle, mode. The on-line performance of SRF cavities can be negatively impacted by the gradual reduction in the accelerating gradient that can be attained within a reasonable field emission level. Conventional cleaning procedures are both time- and resource-exhaustive as they are done *ex-situ*. Plasma processing is an emerging *in-situ* method of cleaning which chemically removes hydrocarbon-based field emitters through plasma. An R&D program is underway at TRIUMF with the goal to develop fundamental power coupler (FPC) driven plasma processing of the installed 1.3 GHz nine-cell cavities in the ARIEL 30 MeV SRF eLINAC. Processing recipes have been systematically studied in single-cell and multi-cell cavities off-line. The progress on these developments will be reported.

INTRODUCTION

TRIUMF's Advanced Rare IsotopE Laboratory (ARIEL) program includes a 3 mA, 30 MeV SRF electron linear accelerator (eLINAC) operating in continuous wave (cw) as a driver to produce radioactive ions through photo-fission [1,2]. The eLINAC consists of three 1.3 GHz nine-cell ARIEL cavities housed in two cryomodules; one within an "injector" module, and the remaining two residing in an "accelerator" cryomodule. Each cavity is specified to operate at a minimum accelerating gradient of 10 MV/m to achieve a threshold Rare Isotope Beam (RIB) production energy of 30 MeV.

The yield of the photo fission process is highly dependent on the electron energy, as seen in Fig. 1. Reductions in the cavity gradient significantly decrease RIB yield and must be avoided. Particulate contamination therefore poses a serious concern for operational efficiency. Field emitters reduce cavity performance through local heating effects and radiation emission, degrading the quality factor of the affected cavity.

Various techniques have been developed to mitigate field emission, but each suffer from some intrinsic limitation. Either large resource and time allocation is needed as they are done *ex-situ*, or they are insufficient at removing hydrocarbon contamination. Plasma processing is an *in-situ* cleaning technique that has been demonstrated to be effective for a number of linac facilities [4,5,6]. Plasma processing utilizes a mixture of an inert gas (i.e. helium or argon) and a reactive gas, oxygen, in the form of a glow discharge to chemically clean the inner cavity surface.

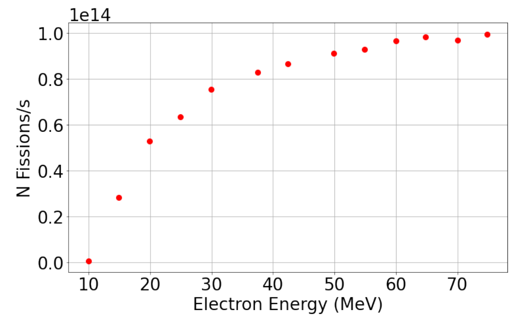

Figure 1: Photo-fission production rates as a function of electron energy for the ARIEL target stations [3].

TRIUMF is pursuing plasma processing for application at the eLINAC to derisk the potential of field emission reducing the available gradient past a point in which RIB yield is compromised. However, ignition through Higher Order Mode (HOM) couplers used in other applications of plasma processing cannot be directly applied on our current configuration. Specifically, the ARIEL cavities are a unique variant of the TESLA design, with modified end groups equipped with two FPCs each. HOM dampers are also utilized at the upstream and downstream beam pipe locations to absorb HOMs [7]. For this reason, we are exploring plasma ignition using FPCs in the TM_{010} passband. In this paper, we will report on our developments in single-cell and multi-cell structures.

METHODS

The apparatus is shown in Fig. 2. A gas supply system continuously injects the process gasses into the cavity, while a pumping system is used to remove byproducts from the plasma reaction. In addition, an RF system is used to excite the cavity fields to strike a plasma at a mode-dependent location. Figure 3 shows an example of a plasma generated within a 1.3 GHz single-cell cavity using this setup.

Gas Supply System

As part of our early studies we have chosen helium as the inert support gas. The gas supply system manages the gas flow within the cavity environment. Gas injection is done using a series of shutoff and leak valves to regulate the percentage of helium gas to oxygen gas, keeping oxygen levels within the range of 5–10%. Total gas pressure within the cavity is measured using a CDG-500 capacitance diaphragm gauge such that total pressure can be regulated to be within the range of 80 mTorr to 200 mTorr.

Content from this work may be used under the terms of the CC BY 4.0 licence (© 2024). Any distribution of this work must maintain attribution to the author(s), title of the work, publisher, and DOI.

ISBN: 978-3-95450-219-6 ISSN: 2226-0366 doi: 10.18429/JACoW-LINAC2024-THPB089

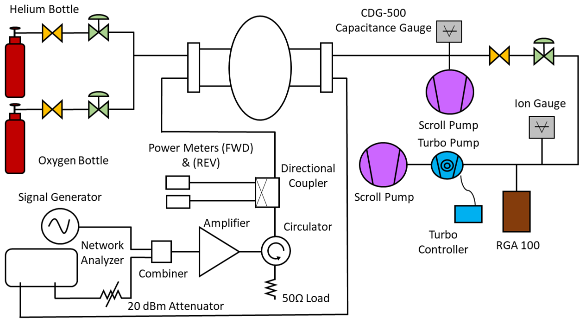

Figure 2: Schematic of the overall plasma processing apparatus. Colored components correlate to the gas supply system, while black and white symbols refer to RF components.

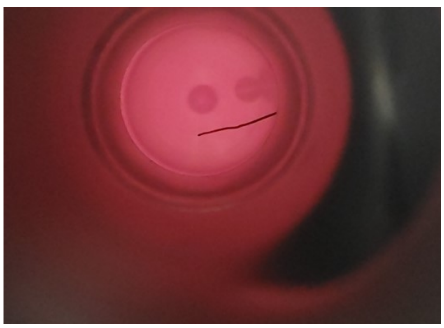

Figure 3: He-O_2 plasma ignited in a 1.3 GHz single cell cavity.

Gas assessment is handled primarily using an SRS100 Residual Gas Analyzer (RGA). The RGA is separated from the primary gas system, and chosen to sample gas from the cavity environment at a pressure of $1 \cdot 10^{-6}$ Torr. In this diagnostic line, the RGA provides real time feedback on process byproducts H_2, H_2O, CO, and CO_2 and He/O_2 ratios, allowing for immediate adjustments to the gas recipe, if necessary.

RF System

The RF system used is inspired by JLab's design [5]. In this particular setup, drive signals from a signal generator are combined with those output from a network analyzer. Here the network analyzer is set to sweep over a frequency range of interest, displaying the S21 response around a certain resonance peak. As plasma density can alter the frequency of a resonant peak, the combined signal tracks plasma responses stemming from drive signal changes. Forward and reflected powers are also tracked during processing.

SINGLE CELL TESTING

To confirm our apparatus and processes could ignite and maintain a plasma capable of cleaning, plasma processing was initially conducted on a 1.3 GHz single cell cavity. The simplicity in the RF structure, and therefore plasma location, made the single cell an ideal first candidate to study plasma characteristics. In total, two types of plasma were ignited

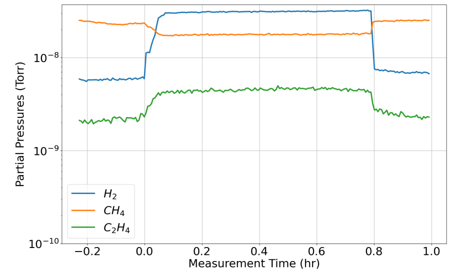

Figure 4: Gas behaviors over time for a contamination plasma. Plasma ignition occurs at $t = 0$, and is held over the duration of the contamination cycle (~45 minutes).

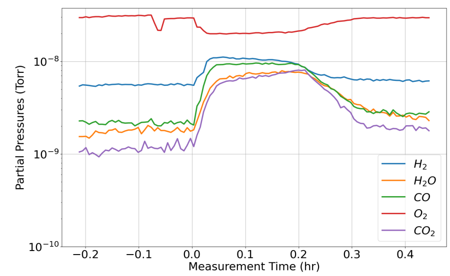

Figure 5: Gas exhaust over time for a cleaning plasma. Of note, plasma ignition is set to be t=0.

within the single cell: a contaminating He−CH_4 plasma, and a cleaning He−O_2 plasma. Fundamentally, the contaminating plasma follows similar cracking principles as the cleaning plasma, except here the aim is to deposit the hydrocarbon molecules onto the cavity's inner surface, rather than removing them from the surface. Methane plasma provides a consistent basis of hydrocarbon contamination across repeated plasma cleaning tests.

Figure 4 shows the gas behavior over the course of a contamination cycle. At plasma ignition, substantial changes can be seen in the byproduct partial pressures. Methane immediately decreases, indicating the breaking of molecular bonds in the volatile plasma environment. New byproduct formations either settle on the cavity surface or are pumped out of the system. Molecules of mass 2, H_2, and mass 28 are seen to be readily pumped out of the cavity space. The increase of mass 28 is suspected to be due to the formation of C_2H_4, instead of a molecule which shares the same atomic mass, like CO or N_2. All partial pressure behaviors subside once RF is halted, with no other anomalous particle combinations being observed otherwise.

Figure 5 showcases the RGA measurements of the cleaning plasma. The results produced are consistent with the expected cleaning procedure. Specifically, once the plasma ignites, a sharp increase is seen with predicted molecules, H_2, H_2O, CO, and CO_2. At this point, the plasma reaction is experiencing the bulk of hydrocarbon contamination, which causes a change in the shown partial pressures. As the cleaning continues, there is a net decay until a steady state is reached, indicating a reduction of hydrocarbons within the cell.

© Content from this work may be used under the terms of the CC BY 4.0 licence (© 2024). Any distribution of this work must maintain attribution to the author(s), title of the work, publisher, and DOI.

ISBN: 978-3-95450-219-6 ISSN: 2226-0366 doi: 10.18429/JACoW-LINAC2024-THPB089

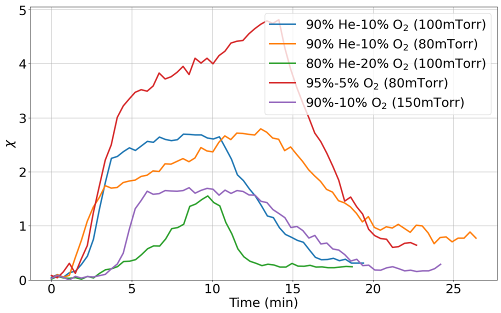

Figure 6: CO_2 peaks for various cleaning recipes. Peaks are normalized using Eq. (1).

Recipe Comparison

In an attempt to optimize the plasma for hydrocarbon removal, several gas recipes were tested to see if parameter changes could influence the abundances of removed byproducts. Plasma cleaning was performed following a standardized contamination step, adjusting the cavity pressure and/or the gas-to-gas ratio. Figure 6 shows the comparison of CO_2 yields produced from the most effective cleaning recipes. Note that these plots were normalized under the scheme

$$\chi = \frac{PP_P - PP_{NP}}{P_{CAV}} \tag{1}$$

to allow for direct comparisons between recipes. Here P_{CAV} is the cavity pressure used during the cleaning step, and PP_P and PP_{NP} are the partial pressures of an observed byproduct when plasma is ignited and extinguished, respectively. Generally, the combination of low cavity pressures with lower oxygen levels produced the highest yields of byproducts, which is in good agreement with recent community developments [8].

Observing the trend of the length of each CO_2 emission peak, there is not a clear answer as to its physical interpretation. At present, we suspect it could be one of two things. Firstly, it is possible that the contamination procedure developed did not equally deposit hydrocarbons across each trial. In short, surface contamination could be removed faster in cases where there is a reduced quantity of hydrocarbons due to the limited number of bonds available for the oxygen. Secondly, the plasma was not sufficient in cracking exotic hydrocarbon chains. Namely, there is a possibility of the contaminating plasma facilitating unlikely hydrocarbon formations, as seen with C_2H_4.

Until now, we have expected hydrocarbon chains to follow the generalized pattern C_xH_y [6]. Whenever a molecule with multiple carbon bonds is created, the bond strength increases, which requires more energy to separate the atoms; for doubly bonded carbon atoms, this energy increases by approximately 56 kJ/mol [9]. If these foreign molecules are more prevalent, the length reduction observed means that the plasma energy is too low to crack the hydrocarbon formations, rendering it difficult to fully clean the inner cavity surface. Further testing is required before a firm consensus can be made.

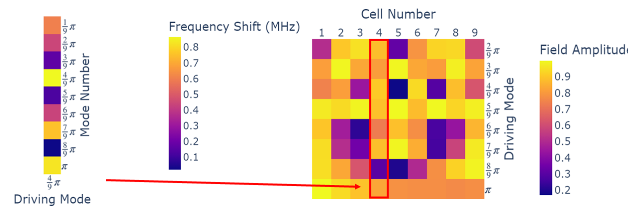

Figure 7: Resonant frequency shifts (left) and beadpull data (right) across a 1.3 GHz 9-cell TESLA cavity driven in the $4\pi/9$ mode.

MULTI-CELL TESTING

Transitioning into multi-cell plasma processing adds a new level of complexity through variation in plasma location. At this stage in testing we are attempting to formulate a mode ignition procedure to sequentially clean each of the cells within a 1.3-GHz 9-cell TESLA cavity. To do this, frequency shifts in each resonant mode have been measured. Comparisons are currently being made with beadpull measurements of mode in the fundamental bandpass to estimate the physical locations of plasma within the cavity. The dielectric changes created by plasma in the cavity can be treated as a perturbation, and thus related to the beadpull data through a normalization constant.

Figure 7 shows an example of the outlined comparison between the described measurement sets when the cavity is being driven in the $4\pi/9$ mode; the data is arranged following the SNS format [4]. Here, the grid format allows for a convenient visual matching of the experimental findings with mode-specific electric field regions that are used to ignite the plasma. In the example provided, the mode shifts best align with the beadpull behavior seen with the fourth cell.

An interesting feature is that when igniting plasma in the $7\pi/9$, $8\pi/9$, and π modes, we noticed that in each case, the $7\pi/9$ mode disappears. What is left is eight of the initial nine modes, with the $6\pi/9$ mode filling the space previously occupied by the two modes. This results in a substantial increase in the sixth mode's frequency shift, skewing the comparison between the two models.

OUTLOOK

Plasma processing has been performed and validated on a 1.3 GHz single-cell SRF cavity. By varying plasma parameters, we have improved our plasma's effectiveness at the removal of byproducts. However, single cell testing was only the first hurdle out of many needed to confidently apply plasma processing on ARIEL's cryomodules. Cold tests using a single-cell cavity are currently being conducted to qualify plasma processing. The next stage of TRIUMF's plasma processing endeavors will focus solely on multi-cell structures.

© Content from this work may be used under the terms of the CC BY 4.0 licence (© 2024). Any distribution of this work must maintain attribution to the author(s), title of the work, publisher, and DOI.

ISBN: 978-3-95450-219-6 ISSN: 2226-0366 doi: 10.18429/JACoW-LINAC2024-THPB089

Content from this work may be used under the terms of the CC BY 4.0 licence (© 2024). Any distribution of this work must maintain attribution to the author(s), title of the work, publisher, and DOI.

REFERENCES

[1] J. A. Bagger *et al.*,"ARIEL at TRIUMF: Science and Technology", in *Proc. IPAC'18*, Vancouver, Canada, Apr. 2018, pp. 6–11. doi:10.18429/JACoW-IPAC2018-MOXGB2

[2] R. E. Laxdal *et al.*, "The 30-MeV Stage of the ARIEL e-Linac",in *Proc. SRF'17*, Lanzhou, China, Jul. 2017, pp. 6–12. doi:10.18429/JACoW-SRF2017-MOXA03

[3] P. G. Bricault *et al.*, "Progress Towards New RIB and Higher Intensities at TRIUMF", in *Proc. Cyclotrons'10*, Lanzhou, China, Sep. 2010, pp. 365–370.

[4] M. Doleans *et al.*, "Plasma Processing R&D for the SNS Superconducting Linac RF Cavities", in *Proc. SRF'13*, Paris, France, Sep. 2013, paper TUP057, pp. 551–557.

[5] T. Powers, N. C. Brock, and T. D. Ganey, "In-Situ Plasma Processing of Superconducting Cavities at Jefferson Lab", in *Proc. SRF'21*, East Lansing, MI, USA, Jun. 2021, p. 485. doi:10.18429/JACoW-SRF2021-TUPTEV004

[6] B. Giaccone *et al.*, "Plasma Processing to Reduce Field Emission in LCLS-II 1.3 GHz SRF Cavities", in *Proc. SRF'19*, Dresden, Germany, Jun. 2019, pp. 1231–1238. doi:10.18429/JACoW-SRF2019-FRCAB7

[7] P. Kolb, "The TRIUMF Nine-Cell SRF Cavity for ARIEL", PhD. thesis, University of British Columbia, British Columbia, Canada, 2016.

[8] T. Powers, N. C. Brock, and T. D. Ganey, "In Situ Plasma Processing of Superconducting Cavities at JLab, 2023 Update", in *Proc. SRF'23*, Grand Rapids, MI, USA, Jun. 2023, pp. 701–705. doi:10.18429/JACoW-SRF2023-WEPWB054

[9] S. J. Blanksby and E. G. Barney, "Bond Dissociation Energies of Organic Molecules", in *Accounts of Chemical Research*, vol. 36, issue 4, Jan. 2003. doi:10.1021/ar020230d